Biochimica et Biophysica Acta 1813 (2011) 2061–2070

Contents lists available at ScienceDirect

Biochimica et Biophysica Acta

journal homepage: www.elsevier.com/locate/bbamcr

Periostin mediates human adipose tissue-derived mesenchymal stem cell-stimulated tumor growth in a xenograft lung adenocarcinoma model

Soon Chul Heo [a,b,1], Kook One Lee [f,g,1], Sang Hun Shin [a,b], Yang Woo Kwon [a,b], Young Mi Kim [b], Chang Hun Lee [c], Yeong Dae Kim [d], Min Ki Lee [e], Man-Soo Yoon [f], Jae Ho Kim [a,b,g,*]

[a] Medical Research Center for Ischemic Tissue Regeneration, Pusan National University, Yangsan, Republic of Korea
[b] Department of Physiology, School of Medicine, Pusan National University, Yangsan, Republic of Korea
[c] Department of Pathology, School of Medicine, Pusan National University, Yangsan, Republic of Korea
[d] Department of Thoracic Surgery, School of Medicine, Pusan National University, Yangsan, Republic of Korea
[e] Department of Internal Medicine, School of Medicine, Pusan National University, Yangsan, Republic of Korea
[f] Department of Obstetrics and Gynecology, School of Medicine, Pusan National University, Yangsan, Republic of Korea
[g] Research Institute of Convergence of Biomedical Science and Technology, Pusan National University Yangsan Hospital, Yangsan, Republic of Korea

ARTICLE INFO

Article history:
Received 7 May 2011
Received in revised form 22 July 2011
Accepted 3 August 2011
Available online 10 August 2011

Keywords:
Periostin
Lysophosphatidic acid
Mesenchymal stem cells
Adhesion
Tumorigenesis

ABSTRACT

Mesenchymal stem cells stimulate tumor growth *in vivo* through a lysophosphatidic acid (LPA)-dependent mechanism. However, the molecular mechanism by which mesenchymal stem cells stimulate tumorigenesis is largely elusive. In the present study, we demonstrate that conditioned medium from A549 human lung adenocarcinoma cells (A549 CM) induces expression of periostin, an extracellular matrix protein, in human adipose tissue-derived mesenchymal stem cells (hASCs). A549 CM-stimulated periostin expression was abrogated by pretreatment of hASCs with the LPA receptor 1 (LPA_1) inhibitor Ki16425 or short hairpin RNA-mediated silencing of LPA_1, suggesting a key role of the LPA–LPA_1 signaling axis in A549 CM-stimulated periostin expression. Using a xenograft transplantation model of A549 cells, we demonstrated that co-injection of hASCs potentiated tumor growth of A549 cells *in vivo* and that co-transplanted hASCs expressed not only periostin but also α-smooth muscle actin (α-SMA), a marker of carcinoma-associated fibroblasts. Small interfering RNA- or short hairpin RNA-mediated silencing of periostin resulted in blockade of LPA-induced α-SMA expression in hASCs. In addition, silencing of periostin resulted in blockade of hASC-stimulated growth of A549 xenograft tumors and *in vivo* differentiation of transplanted hASCs to α-SMA-positive carcinoma-associated fibroblasts. Conditioned medium derived from LPA-treated hASCs (LPA CM) potentiated proliferation and adhesion of A549 cells and short interfering RNA-mediated silencing or immunodepletion of periostin from LPA CM abrogated proliferation and adhesion of A549 cells. These results suggest a pivotal role for hASC-secreted periostin in growth of A549 xenograft tumors within the tumor microenvironment.

1. Introduction

Tumors are composed of neoplastic cells and non-neoplastic stromal cell components, including fibroblasts, myofibroblasts, endothelial cells, pericytes, and inflammatory cells [1]. Carcinoma-associated fibroblasts (CAFs, also known as myofibroblasts or cancer stroma), which express α-smooth muscle actin (α-SMA) as a phenotypic marker, have been shown to play important roles during cancer progression and metastasis [2,3]. They stimulate tumorigenesis, angiogenesis, and invasion in a variety of solid tumors, including prostate, breast, and ovarian carcinomas [1,4–7] by secretion of various extracellular matrix proteins, proteases, chemokines, and angiogenic factors [8]. Co-transplantation of CAFs has been shown to stimulate invasiveness of prostate and breast tumors in a xenograft tumor model [6,7]. CAFs have been reported to originate from various cell types, including tissue-resident fibroblasts, cancer cells or epithelial cells undergoing epithelial-to-mesenchymal transition, or mesenchymal stem cells [2].

Mesenchymal stem cells (MSCs) have a capacity for self-renewal, long-term viability, and differentiation potential toward diverse cell types, including adipogenic, osteogenic, chondrogenic, and myogenic lineages [9–12], suggesting clinical usefulness of MSCs for tissue

Abbreviations: α-SMA, α-smooth muscle actin; A549 CM, conditioned medium from A549 cells; CAFs, carcinoma-associated fibroblasts; CM-DiI, chloromethylbenzamide-1,1′-diactaolecyl-3,3,3′,3′-tetramethylindocarbocyanine perchlorate; DAPI, 4′,6-diamidino-2-phenylindole; GAPDH, glyceraldehydes-3-phosphate dehydrogenase; hASCs, human adipose tissue-derived mesenchymal stem cells; LPA, lysophosphatidic acid; MSCs, mesenchymal stem cells; LPA CM, conditioned medium from LPA-treated hASCs; siRNA, small interfering RNA; shRNA, short hairpin RNA; TGF-β1, transforming growth factor-β1

* Corresponding author at: Department of Physiology, School of Medicine, Pusan National University, Yangsan 626-870, Gyeongsangnam-do, Republic of Korea. Tel.: +82 51 510 8073; fax: +82 51 510 8076.
E-mail address: jhkimst@pusan.ac.kr (J.H. Kim).

[1] These authors contributed equally to this work.

0167-4889/$ – see front matter © 2011 Elsevier B.V. All rights reserved.
doi:10.1016/j.bbamcr.2011.08.004

regeneration. MSCs are distributed in bone marrow and many other peripheral tissues where they are thought to serve as local sources of tissue-resident stem cells [13]. In addition, recruitment of bone marrow-derived MSCs into the stroma of developing tumors has been reported [14]. MSCs constitute a large proportion of non-neoplastic stromal cells within the tumor microenvironment [2]. Accumulating evidence suggests that MSCs have an adverse effect that favors tumor growth: when transplanted subcutaneously, tumor cells mixed with MSCs exhibited elevated capability of proliferation and rich angiogenesis in tumor tissues [15]. In addition, MSCs co-injected with human breast carcinoma cells into a subcutaneous site by xenograft transplantation stimulated metastatic potency of breast carcinoma [16]. Furthermore, human bone marrow-derived MSCs exposed to tumor-conditioned medium have been reported to exhibit phenotypic characteristics and ability of CAFs in promotion of tumor cell growth *in vitro* and in an *in vivo* co-implantation model [17]. These results suggest regulation of tumor growth and metastasis *in vivo* through paracrine crosstalk between MSCs and cancer cells.

Lysophosphatidic acid (LPA) is a small bioactive phospholipid produced by activated platelets, mesothelial cells, fibroblasts, adipocytes, and some cancer cells [18–20]. Accumulating evidence suggests that LPA is implicated in tumorigenesis and metastasis [19]. We have previously reported that LPA induced migration of human adipose tissue-derived MSCs (hASCs) and stimulated differentiation of cells to α-SMA-positive CAFs [21,22], suggesting a pivotal role of LPA in generation of CAFs within the tumor microenvironment. Co-transplantation of hASCs with A549 human lung adenocarcinoma stimulated growth of xenograft tumors *in vivo* and short hairpin RNA (shRNA)-mediated silencing of LPA receptor 1 (LPA_1) in hASCs abrogated hASC-stimulated *in vivo* growth of A549 xenograft tumors [23]. In addition, conditioned medium from A549 cells (A549 CM) contained significant levels of LPA and elicited differentiation of hASCs to α-SMA-positive CAFs through an LPA_1-dependent mechanism *in vitro* [23]. These results suggest that hASCs can be differentiated to α-SMA-positive CAFs through an LPA–LPA_1-dependent mechanism within the tumor microenvironment. However, the molecular mechanisms by which hASCs stimulate *in vivo* growth of A549 xenograft tumors are still elusive.

Periostin, originally named osteoblast-specific factor-2, is a disulfide-linked 90-kDa secretory protein that functions as a cell adhesion molecule. It shares a structural homology to insect fasciclin I and supports adhesion of osteoblasts, thereby functioning in recruitment and attachment of osteoblasts to the periosteum [24]. In addition to its role in bone physiology, accumulating evidence has demonstrated involvement of periostin in tumor growth and survival, angiogenesis, and metastasis [25]: high expression of periostin has been associated with tumor size, lymph node metastasis, disease stage, and lymphatic invasion in non-small cell lung cancer patients [26]. Furthermore, over-expression of periostin in patients with lung cancer has been correlated with clinicopathological data, including squamous cell carcinoma type, higher stage, vessel infiltration, and tumor relapse [27]. Ectopic over-expression of periostin promoted proliferation and migration of A549 cells *in vitro* [28]. We previously reported on high expression of periostin in CAFs of epithelial ovarian cancer tissues [29]. In addition, conditioned medium from ovarian cancer cells stimulated expression of not only α-SMA but also periostin in hASCs through an LPA_1-dependent mechanism [29], implying a possible role of periostin as an hASC-derived paracrine factor. However, involvement of hASC-secreted periostin in tumorigenesis has not been explored.

In order to clarify the paracrine mechanisms involved in the crosstalk between cancer cells and hASCs, we explored the role of hASC-secreted periostin in tumor growth using an *in vivo* xenograft co-transplantation model of A549 cells. The present study demonstrates for the first time that periostin plays a pivotal role in adhesion and proliferation of A549 cells as a paracrine factor secreted from hASCs.

2. Materials and methods

2.1. Materials

Trypsin, α-minimum essential medium, fetal bovine serum, Alexa Fluor 488 goat anti-rabbit, and Alexa Fluor 647 goat anti-mouse antibodies were purchased from Invitrogen (Carlsbad, CA, http://www.invitrogen.com). Anti-glyceraldehyde-3-phosphate dehydrogenase (GAPDH) antibody was purchased from Millipore (Temecula, CA, http://www.milliore.com). 1-Oleoyl-*sn*-glycero-3-phosphate (LPA), Ki16425, and anti-α-SMA antibody were purchased from Sigma-Aldrich (St. Louis, MO, http://www.sigmaaldrich.com). Anti-periostin antibody was purchased from Abcam (Cambridge, MA). Recombinant human periostin was purchased from R&D Systems, Inc. (Minneapolis, MN, http://www.rndsystems.com). Vectashield mounting medium with 4′-6-Diamidino-2-phenylindole (DAPI) was purchased from Vector Laboratories (Burlingame, CA, http://vectorlabs.com). Culture plates were purchased from Nunc (Roskilde, Denmark, http://www.nuncbrand.com). Peroxidase-labeled secondary antibodies and system were purchased from Amersham Biosciences (Pittsburgh, PA, http://www4.gelifesciences.com).

2.2. Cell culture

hASCs were isolated from subcutaneous adipose tissues, which were obtained from elective surgeries with patient's consent as approved by the Institutional Review Board of Pusan National University Hospital. For isolation of hASCs, adipose tissues were washed at least three times with sterile PBS and treated with an equal volume of collagenase type I suspension (1 g/l of HBSS buffer with 1% bovine serum albumin) for 60 min at 37 °C with intermittent shaking. Floating adipocytes were separated from the stromal–vascular fraction by centrifugation at 300×*g* for 5 min. The cell pellet was re-suspended in α-minimum essential medium supplemented with 10% fetal bovine serum, 100 U/ml penicillin, and 100 μg/ml streptomycin and cells were plated in tissue culture dishes at 3500 cells/cm^2. Primary hASCs were cultured for 4–5 days until they reached confluence and were defined as passage "0". The passage number of hASCs used in these experiments was 3–10. Human lung adenocarcinoma A549 cells were obtained from the American Tissue Type Culture (Rockville, MD, http://www.atcc.org) and maintained in RPMI medium supplemented with 10% FBS at 37 °C.

2.3. Preparation of conditioned medium

For preparation of conditioned medium from A549 cells, cells were seeded on 100-mm cell culture dishes and cultured in growth medium until reaching confluence. Cells were briefly rinsed twice with PBS, followed by incubation with 10 ml of serum-free α-minimum essential medium for 48 h prior to collection of culture medium. For collection of conditioned medium from hASCs, cells were treated with fresh serum-free α-minimum essential medium containing vehicles or LPA for 48 h. Culture supernatants were centrifuged at 2000 rpm for 10 min for removal of cell debris, followed by filtering with 0.45 μm Millipore syringe filters (Millipore, Bedford, MA), and storage at −70 °C for subsequent use.

2.4. Cell adhesion and proliferation assays

To explore the effect of periostin on adhesion ability of A549 cells, ninety six-well microculture plates (Falcon, Becton-Dickinson, Mountain View, CA) were incubated with recombinant periostin proteins at 37 °C for 12 h, followed by blocking with PBS containing 0.2% BSA for 1 h at 37 °C. A549 cells were trypsinized and suspended in the culture media at a density of 2×10^5 cells/ml, and 0.1 ml of the cell suspension was then added to each well of the plates. Following incubation for 1 h at 37 °C, unattached cells were removed by rinsing twice with PBS. Cells were

counted under microscopy at ×100 magnification after staining with hematoxylin and eosin for determination of the number of attached cells.

To explore the effects of recombinant periostin or conditioned medium from hASCs on cell proliferation of A549 cells, a colorimetric 3-(4,5-dimethylthiazol-2-yl)-2,5-diphenyltetrazolium bromide (MTT) assay was used: MTT is metabolized by NAD-dependent dehydrogenase to form a colored reaction product (formazan), and the amount of dye formed correlates directly with the number of cells. For determination of cell numbers, hASCs were seeded in a 24-well culture plate at a density of 2×10^4 cells/well, cultured for 48 h in normal growth medium, serum-starved for 24 h, and treated with various reagents (or a vehicle control) for the indicated times. Cells were washed twice with PBS and incubated with 100 μl of MTT (0.5 mg/ml) for 2 h at 37 °C. Formazan granules generated by the cells were dissolved in 100 μl of dimethylsulfoxide, and the absorbance of the solution at 562 nm was determined using a $PowerWave_x$ microplate spectrophotometer (Bio-Tek Instruments, Inc.; Winooski, VT) after dilution to a linear range.

2.5. Western blotting

Expression levels of α-SMA and periostin were determined by Western blotting analysis. Serum-starved hASCs were treated with appropriate conditions, washed with ice-cold PBS, and then lysed in lysis buffer (20 mM Tris–HCl, 1 mM EGTA, 1 mM EDTA, 10 mM NaCl, 0.1 mM phenylmethylsulfonyl fluoride, 1 mM Na_3VO_4, 30 mM sodium pyrophosphate, 25 mM β-glycerol phosphate, 1% Triton X-100, pH 7.4). Lysates were resolved by SDS-PAGE, transferred onto a nitrocellulose membrane, and then stained with 0.1% Ponceau S solution (Sigma-Aldrich). After blocking with 5% nonfat milk, the membranes were immunoblotted with various antibodies, and bound antibodies were visualized with horseradish peroxidase-conjugated secondary antibodies using the enhanced chemiluminescence Western blotting system (ECL, Amersham Biosciences).

2.6. Gene silencing using shRNA lentivirus or small interfering RNA (siRNA)

cpLKO.1-puro lentiviral vectors expressing LPA_1 shRNA (TRCN0000011368), periostin shRNA (TRCN0000123054), and non-target control shRNA (SHC002) were purchased from Sigma-Aldrich. Functional sequences in the shRNA vectors are as follows: LPA_1, "CCGGCCTTCTGAAGACTGTGGTCATCTCGAGATGACCACAGTCTTCAGAAGGTTTTT" to target the LPA_1 gene sequence (CCTTCTGAAGACTGTGGTCAT); sh-periostin, "CCGGCGAGCCTTGTATGTATGTTATCTCGAGATAACATACATACAAGGCTCGTTTTTG" to target the periostin gene sequence (CGAGCCTTGTATGTATGTTAT). For generation of lentiviral particles, HEK293FT cells were co-transfected with the shRNA lentiviral plasmid (pLKO.1-puro) and ViraPower Lentiviral packaging mix (pLP1, pLP2, pLP-VSV-G; Invitrogen) using Lipofectamine 2000 (Invitrogen) and culture supernatants containing lentivirus were harvested at 48 h after transfection. For lentiviral transduction, hASCs were treated with culture supernatants from HEK293FT cells in the presence of 5 μg/ml polybrene (Sigma-Aldrich) and stable cell lines expressing shRNA were generated by selection with puromycin (5 μg/ml). To ensure shRNA-mediated silencing of LPA_1 and periostin expression, mRNA levels of LPA_1, periostin, and GAPDH were determined by RT-PCR analysis.

For siRNA experiments, hASCs were seeded on 60 mm-diameter dishes. At 70% confluence, cells were transfected with appropriate siRNAs using Lipofectamine 2000 reagent according to the manufacturer's instructions (Invitrogen). Periostin siRNA duplexes were synthesized, desalted, and purified by Samchully Pharm. Co. Ltd. (Siheung, GyeongGi, Korea) as follows: periostin 5′-CCGAAGCUCUUAUGAAGUATT-3′ (sense) and 5′-UACUUCAUAAGAGCUUCGGTT-3′ (anti-sense). Nonspecific control siRNA was purchased from Dharmacon (Lafayette, CO). Lipofectamine 2000 reagent was incubated with serum-free medium for 10 min, followed by addition of respective siRNAs to the mixtures. After incubation for 15 min at room temperature, the mixtures were diluted with serum-free medium and added to each well to a final concentration of 100 nM. Following incubation of hASCs with siRNAs for 6 h, the cells were cultured in growth medium for 24 h, and expression levels of periostin and GAPDH were determined by Western blotting.

2.7. In vivo xenograft tumorigenesis model

BALB/c–nu/nu mice were randomly divided into three groups (nine mice in each group). hASCs were labeled with the fluorescent cell surface marker chloromethylbenzamide-1,1′-diactaolecyl-3,3,3′,3′-tetramethylindocarbocyanine perchlorate (CM-Dil) (Invitrogen, Carlsbad, CA, http://probes.invitrogen.com) prior to transplantation. Mice received subcutaneous administration of A549 cells (1×10^6 cells/60 μl PBS) alone or mixed with hASCs (1×10^6 hASCs plus 1×10^6 A549 cells/60 μl PBS) into the front of the backside. Mice were examined 2 times per week, and tumor volume was evaluated by measurement of the length and width of the tumor mass in millimeters (mm) using electronic vernier calipers. Tumor volume (mm^3) was calculated using the formula $V = (\text{length}\times\text{width}\times\text{width})/2$. After 4 weeks, mice were sacrificed, and weights of xenograft tumors were quantified.

2.8. Immunostaining and analysis of images

Immunohistochemistry was performed using the streptavidin–peroxidase technique and the DAKO EnVision System (Dako Cytomation, Hamburg, Germany). Consecutive paraffin-embedded tissue sections (2.5-μm thick) were deparaffinized and rehydrated. For antigen retrieval, slides were pretreated in citrate buffer (pH 6.0) in a microwave oven for 12 min. Slides were then cooled to room temperature in deionized water for 5 min. Endogenous peroxidase activity was quenched by incubation of the slides in methanol containing 0.3% hydrogen peroxide, followed by washing with deionized water for 3 min, after which the sections were incubated for 1 h at room temperature with normal goat serum, and subsequently incubated at room temperature for 1 h with the primary anti-α-SMA (Sigma; 1:200 dilution) antibody. Next, the sections were rinsed with washing buffer (PBS containing 0.5% Tween 20) and incubated with biotinylated anti-mouse IgG and streptavidin–peroxidase complex, followed by reaction with diaminobenzidine and counterstaining with Mayer's hematoxylin. In addition, to confirm the specificity of the primary antibody and the technique used, tissue sections were incubated in the absence of the primary antibody and with negative control IgG. Under these conditions, no specific immunostaining was detected.

Immunostaining and confocal microscopy were used for determination of the cellular expression patterns of proteins within xenograft tumor tissues. For immunostaining, specimens were incubated with anti-α-SMA or anti-periostin antibodies for 2 h, followed by incubation with Alexa Fluor 488-conjugated anti-rabbit or Alexa Fluor 647-conjugated anti-mouse secondary antibodies (Molecular Probes) for 1 h. The specimens were finally washed and mounted in Vectashield medium with DAPI for visualization of nuclei. A Leica TCL-SP2 confocal microscope system was used for collection of images of CM-Dil-, periostin-, or α-SMA-positive cells and DAPI-positive nuclei. Images of four random non-overlapping microscopic fields of view per xenograft tumor were captured at high power magnification (400×). Using the co-localization Finder plugin of Image J software (NIH, http://rsb.info.nih.gov/ij/plugins/colocalization.html), we measured α-SMA-positive and CM-Dil-positive areas in the images. Relative percentages of α-SMA-positive cells *versus* CM-Dil-positive cells were calculated as percentages of the CM-Dil-positive area.

2.9. Statistical analysis

Results of multiple observations are presented as mean ± SD. Student's *t* test was used for analysis of differences between the two

groups. For multivariate data analysis, one- or two-way ANOVA was used for assessment of group differences, followed by *post hoc* comparison test using Scheffe's method.

3. Results

3.1. A549 CM stimulates expression of periostin in hASCs through an LPA–LPA$_1$-dependent mechanism

LPA–LPA$_1$-dependent paracrine signaling played a key role in differentiation of hASCs to α-SMA-positive CAFs in an *in vivo* xenograft co-transplantation model of A549 cancer cells and hASCs [21,23]. In order to determine whether paracrine signaling from A549 cells can regulate periostin expression in hASCs, we examined expression levels of periostin after exposure of cells to A549 CM for 4 days. As shown in Fig. 1A, A549 CM induced a dose-dependent increase of the expression levels of not only α-SMA but also periostin in hASCs, suggesting that A549-derived paracrine factors stimulate periostin expression in hASCs. To determine whether LPA is responsible for A549 CM-stimulated periostin expression, we examined the effect of LPA on the expression levels of periostin in hASCs. As shown in Fig. 1B, expression levels of both periostin and α-SMA showed a dose-dependent increase by exposure of the cells to LPA, with maximal stimulation at 10 μM concentration. LPA treatment resulted in time-dependent augmentation of the expression levels of periostin and α-SMA, with maximal stimulation on day 4. Of particular interest, LPA-induced periostin expression was detected at 6 h after exposure of hASCs to LPA, while increased α-SMA expression was observed after LPA treatment for 2 days (Fig. 1C), suggesting that periostin expression occurred in advance of α-SMA expression. In order to determine whether LPA is involved in A549 CM-induced periostin expression, we examined the effects of Ki16425, an antagonist specific to LPA$_{1/3}$ receptors, on periostin expression induced by LPA and A549 CM. As shown in Fig. 1D, treatment of cells with 1 μM Ki16425 resulted in complete abrogation of the expression levels of both α-SMA and periostin, which were stimulated by LPA and A549 CM. To further support these results, we depleted endogenous LPA$_1$/EDG$_2$, a major isoform of LPA receptors expressed in hASCs [30], using shRNA lentivirus. As shown in Fig. 1E, LPA$_1$ shRNA attenuated expression of α-SMA and periostin induced by either LPA or A549 CM. These results suggest a key role of the LPA–LPA$_1$ signaling pathway in A549 CM-induced expression of not only α-SMA but also periostin in hASCs.

3.2. Periostin is involved in LPA-induced α-SMA expression in hASCs

For determination of whether periostin is involved in LPA-stimulated α-SMA expression, we examined the effects of siRNA- or shRNA-mediated depletion of endogenous periostin on LPA-induced α-SMA expression. LPA-stimulated periostin expression was abrogated by siRNA transfection or shRNA lentiviral transduction (Fig. 2A and B). Of particular interest, LPA-stimulated α-SMA expression was also blocked by siRNA- or shRNA-mediated silencing of periostin

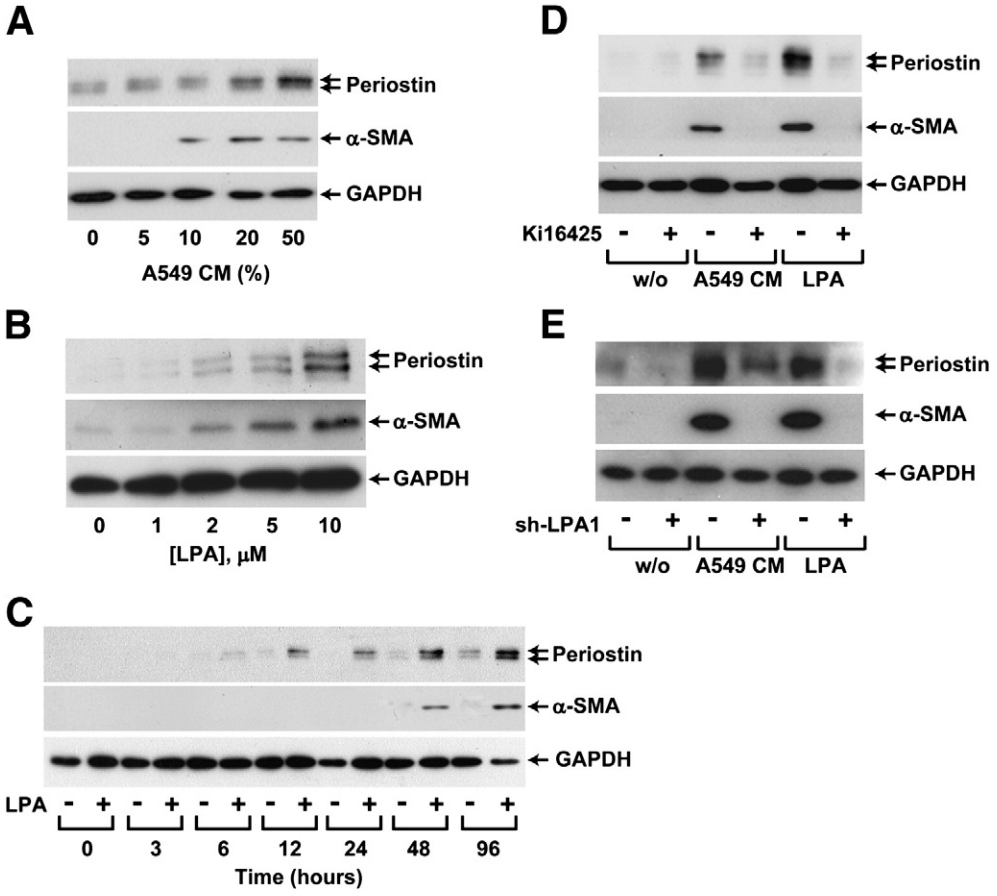

Fig. 1. A549 CM stimulates expression of periostin and α-SMA in hASCs through an LPA–LPA$_1$-dependent mechanism. (A) Serum-starved hASCs were exposed to increasing concentrations of A549 CM for 4 days. (B) Serum-starved hASCs were treated with indicated concentrations of LPA for 4 days. (C) Serum-starved hASCs were treated with vehicle (0.1% fatty acid-free BSA) or 10 μM LPA for the indicated time periods. (D) Serum-starved hASCs were exposed to 50% A549 CM or 10 μM LPA for 4 days in the presence or absence of 10 μM Ki16425. (E) hASCs were infected with sh-control or sh-LPA$_1$ lentivirus, followed by treatment with 50% A549 CM or 10 μM LPA for 4 days. Expression levels of periostin, α-SMA, and GAPDH were determined by Western blotting. Representative data from three independent experiments are shown.

expression. These results suggest that periostin expression is required for LPA-induced α-SMA expression.

3.3. Periostin is involved in hASC-stimulated in vivo growth of A549 human lung adenocarcinoma cells

hASCs co-transplanted with A549 cells in a xenograft tumor model stimulated proliferation of tumor cells and tumor angiogenesis [23]. In order to explore the role of periostin in hASC-stimulated tumor growth, we depleted periostin expression using shRNA lentivirus, and then performed subcutaneous co-transplantation of the cells with A549 cells in nude mice. As shown in Fig. 3A, xenograft transplantation of A549 cells resulted in formation of tumors, and co-transplantation of A549 cells with control shRNA-infected hASCs (sh-control/hASCs) resulted in a time-dependent increase of growth of xenograft tumors, whereas co-transplantation of periostin shRNA-infected hASCs (sh-periostin/hASCs) with A549 cells did not result in increased tumor volume. Consistently, sh-control/hASCs, but not sh-periostin/hASCs, induced an increase in the weights of A549 xenograft tumors (Fig. 3B–C), suggesting a pivotal role of periostin in hASC-stimulated *in vivo* growth of A549 cells.

3.4. Expression of periostin in hASCs-derived CAFs in xenograft tumor tissues

We have reported on differentiation of co-transplanted hASCs to α-SMA-positive CAFs in A549 xenograft tumors [23]. For determination of whether periostin is involved in differentiation of hASCs to CAFs *in vivo*, we examined expression of α-SMA in xenograft tumors. As shown in Fig. 4A, α-SMA-positive CAFs were detected in tumor tissues generated by xenograft transplantation of A549 cells. An increase in the number of α-SMA-positive cells was observed in xenograft tumors in which sh-control/hASCs were co-transplanted with A549 cells. However, co-transplantation of sh-periostin/hASCs together with A549 cells did not result in an increase in the number of α-SMA-positive cells in xenograft tumors. These results suggest that periostin expression is required for *in vivo* differentiation of hASCs to α-SMA-positive CAFs in xenograft tumor tissues.

For determination of whether periostin is expressed in α-SMA-positive CAFs, we performed immunofluorescence double staining in tumor tissues formed by co-transplantation of A549 cells with hASCs labeled with the fluorescent dye DM-Dil. Co-injection of sh-control/hASCs with A549 cells resulted in detection of α-SMA-positive immunoreactivity primarily in CM-Dil-positive cells adjacent to tumor cells in A549 xenograft tumor tissues, suggesting that hASCs can differentiate to α-SMA-positive CAFs (Fig. 4B). Furthermore, periostin immunoreactivity was mainly detected in both α-SMA-positive and CM-Dil-positive cells. However, CM-Dil-positive hASCs expressed low levels of periostin and α-SMA in tumor tissues generated by injection of sh-periostin/hASCs and A549 cells. To ascertain the results, percentages of α-SMA- and periostin-positive cells in CM-Dil-positive cells were counted. As shown in Fig. 4C, approximately 65% cells of CM-Dil-positive sh-control/hASCs showed high expression of both α-SMA and periostin. In contrast, 33% cells of sh-periostin/hASCs expressed low levels of both α-SMA and periostin. These results suggest that periostin is expressed in α-SMA-positive CAFs derived from hASCs in an A549 xenograft tumor model. To explore the effect of hASC-derived periostin on *in vivo* growth of A549 cells, the relative ratio of the number of A549 cells to the number of hASCs in the xenograft tumor tissues was determined by measuring areas of CM-Dil-negative A549 cells and CM-Dil-positive hASCs. The relative ratio of A549 cells to hASCs in xenograft tumor tissues generated by co-injection of sh-periostin/hASCs and A549 cells was markedly decreased compared with that of A549 cells in tumor tissues transplanted with sh-control/hASCs plus A549 cells (Fig. 4D), while the area of CM-Dil-positive hASCs was not significantly affected by silencing of periostin expression *in vivo* (data not shown). These results suggest that hASC-derived periostin promotes *in vivo* growth of A549 cells.

3.5. LPA-activated hASCs stimulate adhesion and proliferation of A549 cells through a periostin-mediated paracrine mechanism

Periostin has been reported to stimulate adhesion and invasion of various cancer cells, including ovary, breast, colon, and oral cancer cells [23,25]. In order to explore the roles of periostin in tumorigenic potentials of A549 cells, we determined the adhesive capability of A549 cells on periostin-coated dishes. Recombinant periostin induced dose-dependent stimulation of adhesion of A549 cells (Supplementary Fig. 1A). In addition, treatment of A549 cells with periostin stimulated proliferation of A549 cells *in vitro* (Supplementary Fig. 1B). These results suggest that periostin can stimulate tumorigenic potentials of A549 cells by stimulating adhesion and proliferation of tumor cells.

In order to determine whether LPA-activated hASCs promote adhesion and proliferation of A549 cells through a periostin-dependent mechanism, the effects of conditioned medium from LPA-treated hASCs (LPA CM) on adhesion and proliferation of A549 cells were examined. As shown in Fig. 5A, higher levels of periostin protein were detected in LPA CM, compared with conditioned medium from mock-treated hASCs (control CM), and transfection of hASCs with si-periostin resulted in completely abrogated secretion of periostin from hASCs. LPA CM derived from si-control-transfected hASCs stimulated adhesion and proliferation of A549 cells *in vitro* (Fig. 5B and C). However, LPA CM obtained from si-periostin-transfected hASCs did not stimulate adhesion and proliferation of A549 cells. These results suggest that periostin secreted from LPA-activated hASCs promotes adhesion and proliferation of A549 cells.

To further confirm these results, we performed immunodepletion of periostin from LPA CM with anti-periostin antibody and evaluated the effects of periostin-depleted LPA CM on adhesion and proliferation of A549 cells. As shown in Fig. 6A, periostin was specifically immunodepleted from LPA CM with anti-periostin antibody but not with control antibody. Periostin-depleted LPA CM did not stimulate adhesion and proliferation of A549 cells (Fig. 6B and C), in contrast to potent stimulation of adhesion and proliferation of A549 cells by control antibody-treated LPA CM. These results support the suggestion that periostin plays a key role in LPA CM-stimulated adhesion and proliferation of A549 cells.

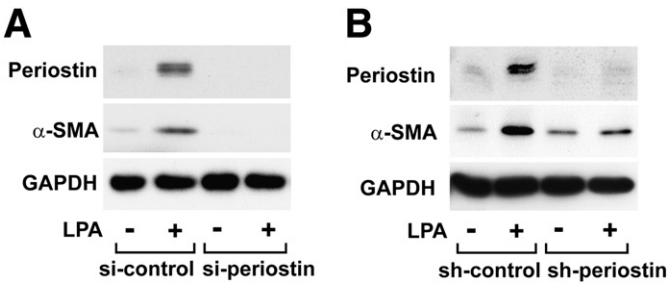

Fig. 2. Role of periostin in LPA-induced α-SMA expression in hASCs. (A) hASCs were transfected with si-control or si-periostin, followed by treatment with 10 μM LPA or vehicles for 4 days. (B) hASCs were infected with sh-control or sh-periostin lentiviruses, followed by treatment with 10 μM LPA or vehicles for 4 days. Expression levels of α-SMA, periostin, and GAPDH were determined by Western blotting. Representative data from three independent experiments are shown.

4. Discussion

In the present study, we demonstrated that A549 CM induced periostin expression in hASCs through an LPA–LPA_1-dependent mechanism. Consistently, we previously reported that conditioned medium

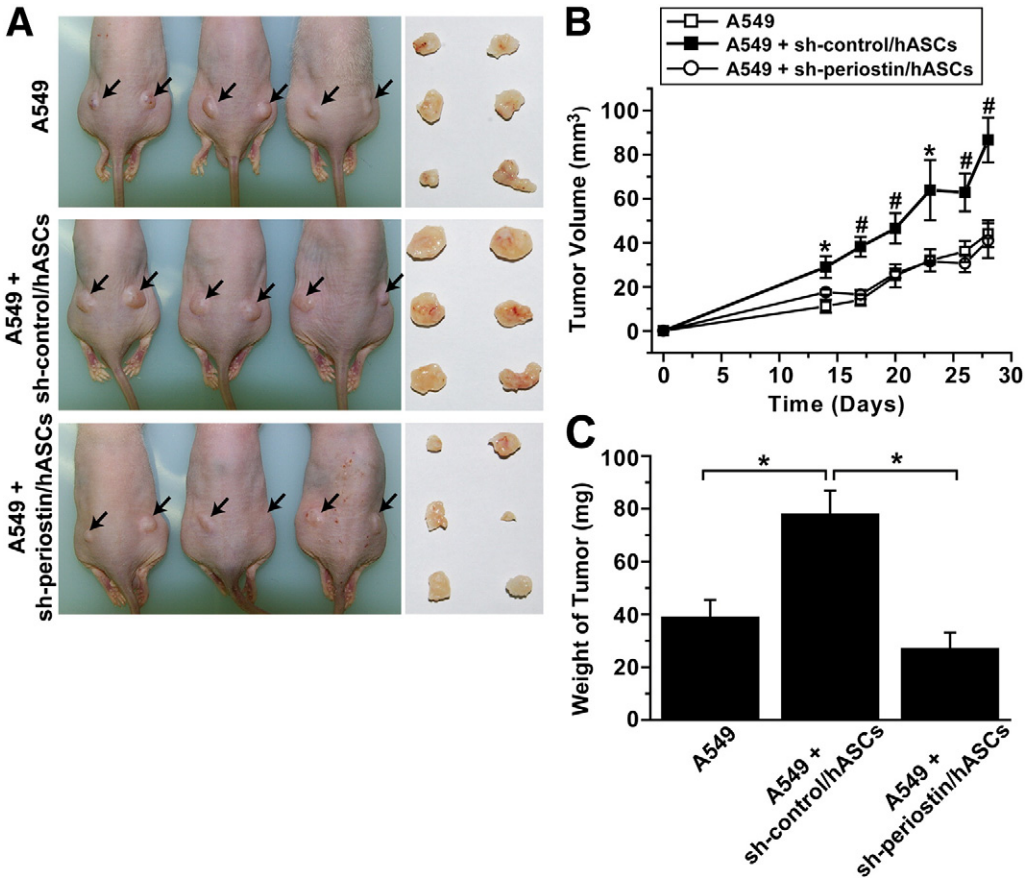

Fig. 3. Role of periostin in hASC-stimulated growth of A549 xenograft tumors. (A) hASCs were infected with sh-control or sh-periostin lentiviruses. A549 cells were injected alone or both A549 cells and lentivirus-infected hASCs were subcutaneously co-injected into nude mice. Mice were then photographed at 4 weeks after injection and xenograft tumors were photographed after sacrifice of mice. (B) Volume of xenograft tumors was measured at the indicated time points. Data are expressed as mean ± SD ($n = 18$). *, $p<0.05$; #, $p<0.01$ *vs* A549 + sh-periostin/hASCs. (C) Weights of the tumor mass were quantified and expressed as mean ± SD ($n = 18$). * indicates $p<0.05$. Representative data from three different experiments are shown.

from ovarian cancer cells, including SK-OV-3 and OVCAR-3, promoted expression of periostin in hASCs [29]. Up-regulation of periostin expression by several extracellular agonists, including TGF-β, BMP-2, IL-4, and IL-13, in different cell types has been reported [31–33]. However, implication of G protein-coupled receptors in regulation of periostin expression is still elusive. LPA exerts its cellular responses through activation of five known G protein-coupled receptors, LPA_{1-5} [34]. In addition to its role in LPA-stimulated periostin expression, LPA_1 mediated LPA-induced migration and differentiation of hASCs to α-SMA-positive CAFs *in vitro* [21–23]. In addition, shRNA-mediated silencing of LPA_1 abrogated LPA-stimulated secretion of angiogenic factors, vascular endothelial growth factors, and stromal cell-derived factor-1α from hASCs *in vitro* [35] and blocked hASC-stimulated tumor angiogenesis *in vivo* [23]. We have reported the existence of LPA in the A549 CM and the concentration of LPA in A549 CM was estimated to be approximately 0.55 ± 0.02 μM [23]. Taken together, these results suggest a key role of LPA_1 in LPA-stimulated pro-tumorigenic responses of hASCs, including differentiation to CAFs, secretion of angiogenic cytokines, and periostin expression.

LPA is generated by the concerted action of multiple enzymes including phospholipase D, diacylglycerol kinase, phospholipase A, autotaxin (also called lysophospholipase D), and monoacylglycerol kinase [18,20,36]. Autotaxin, which was originally identified as a cell motility-stimulating factor from CM of melanoma [37,38]. Enhanced expression of autotaxin has been reported to be associated with increased invasiveness and motility of cancer cells, including breast cancer cells and glioblastoma cells [39,40]. However, we observed that autotaxin mRNA was not detected in A549 cells, whereas hASCs expressed high levels of autotaxin in contrast to lack of LPA in hASC CM [23]. Therefore, it is likely that autotaxin is not responsible for the high levels of LPA in A549 CM, although the mechanisms associated with the high levels of LPA in A549 CM need to be clarified further.

Conditioned medium from tumor cells has been shown to induce differentiation of bone marrow-derived MSCs to α-SMA-positive CAFs [17,41]. Bone marrow-derived MSCs have been reported to contribute to formation of CAFs or myofibroblasts in a mouse pancreatic insulinoma model [42] and in a subcutaneous pancreatic xenograft tumor [43]. In addition, A549 CM promoted *in vivo* and *in vitro* differentiation of hASCs to CAFs expressing α-SMA, VEGF, and SDF-1 through an LPA-mediated mechanism [21,23]. In the present study, we showed that LPA-stimulated periostin expression occurred in advance of α-SMA expression in hASCs (Fig. 1) and silencing of periostin expression using siRNA or shRNA abrogated LPA-stimulated α-SMA expression *in vitro*. In addition, shRNA-mediated depletion of periostin expression abolished differentiation of hASCs to α-SMA-positive CAFs *in vivo*. Periostin was expressed in stromal cells of pancreatic ductal adenocarcinoma and cancer cell supernatants stimulated periostin secretion from pancreatic stellate cells [44]. Recombinant periostin induced an increase in α-SMA, periostin, collagen-1, fibronectin, and TGF-β1 expression in pancreatic stellate cells and siRNA-mediated silencing of endogenous periostin expression resulted in reduced expression of fibronectin, collagen-1, and α-SMA [44]. In contrast to high expression of periostin in hASCs, periostin was not expressed in A549 cells and recombinant periostin did not induce periostin expression in A549 cells (Supplementary Fig. 2). Taken together, these results support the suggestion that LPA-dependent periostin

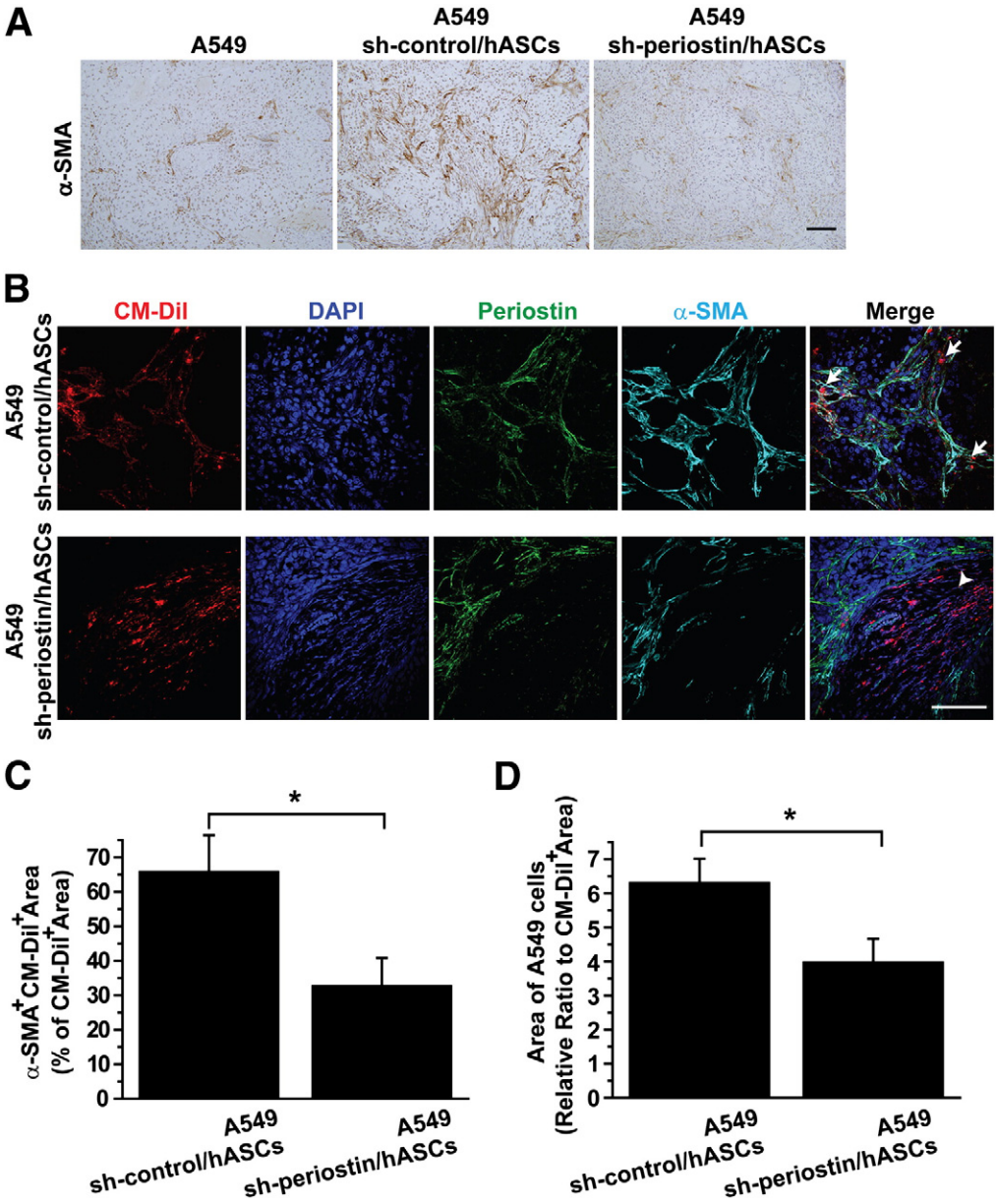

Fig. 4. Role of periostin in differentiation of hASCs to CAFs in xenograft tumor tissues. (A) Expression of α-SMA in xenograft tissues from Fig. 3 were determined by immunostaining. Scale bar = 100 μm. (B) hASCs were labeled with the fluorescent dye CM-DiI prior to co-transplantation with A549 cells into nude mice. Expression of α-SMA and periostin in xenograft tissues was determined by immunostaining. Images of periostin (green color) and α-SMA (cyan color) expression were overlaid with images of hASCs (CM-DiI-positive cells, red color) and nuclei (DAPI, blue color). Arrows indicate co-expression of periostin and α-SMA in CM-DiI-positive cells within tumor tissues transplanted with A549 plus sh-control/hASCs. Arrowheads indicate no expression of periostin and α-SMA in CM-DiI-positive sh-periostin/hASCs co-transplanted with A549 cells. Scale bar = 100 μm. (C) Analysis of α-SMA expression in CM-DiI-positive hASCs in xenograft tumors. Areas of both α-SMA-positive and CM-DiI-positive cells in the images (A549 plus sh-control/hASCs; A549 plus sh-periostin/hASCs) were quantified using Image J software and relative percentages of α-SMA-positive cells in total CM-DiI-positive cells were calculated as described in "Materials and methods". * Indicates $p<0.05$. (n = 18 per each group, 72 fields per group). (D) Quantification of A549 cells in xenograft tumors. Areas of CM-DiI-positive hASCs and CM-DiI-negative A549 cells in the images (A549 plus sh-control/hASCs; A549 plus sh-periostin/hASCs) were quantified using Image J software and relative ratio of A549 cells to hASCs were calculated. * Indicates $p<0.05$.

expression is involved in A549 CM-stimulated differentiation of hASCs to α-SMA-positive CAFs, albeit the molecular mechanism by which periostin stimulates differentiation of hASCs to CAFs should be further clarified.

Bone marrow-derived MSCs have been reported to stimulate tumorigenesis and angiogenesis in xenograft transplantation animal models [15,17]. MSCs have been known to stimulate tumor angiogenesis by secretion of vascular endothelial growth factors in pancreatic carcinoma [45]. Furthermore, MSCs co-injected with human breast carcinoma cells into a subcutaneous site by xenograft transplantation stimulated metastatic potency of breast carcinoma by secretion of chemokine CCL5 [16]. In addition, hASCs stimulated growth and/or metastasis of several cancer cells, including breast, colon, and prostate cancer [46–48]. They stimulated angiogenesis in a VEGF-dependent paracrine fashion and augmented tumor angiogenesis in an A549 xenograft tumor model [23,35]. In the present study, we demonstrated that periostin plays a key role in hASC-stimulated growth of A549 xenograft tumors *in vivo*. Recombinant periostin protein induced an increase in adhesion and proliferation of A549 cells *in vitro*. LPA CM from hASCs promoted adhesion and proliferation of A549 cells through a periostin-dependent mechanism. However, LPA-induced secretion of VEGF and SDF-1 was not affected by silencing of periostin

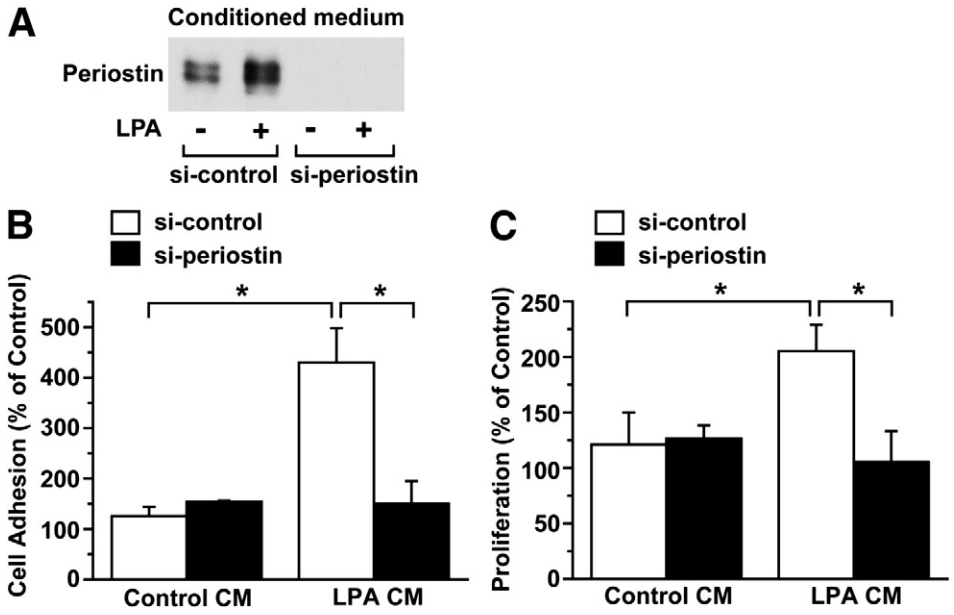

Fig. 5. Effects of siRNA-mediated silencing of periostin expression in LPA CM-stimulated adhesion and proliferation of A549 cells. (A) hASCs were transfected with si-control or si-periostin, followed by treatment with 10 μM LPA or vehicles for 2 days, and protein levels of periostin in LPA CM and control CM were determined by Western blotting. (B) 96-well plates were coated with LPA CM or control CM, and adhesion of A549 cells onto the plates was determined. (C) A549 cells were treated with 50% control CM or LPA CM for 4 days and proliferation of A549 cells was determined. Data are expressed as mean ± SD (n = 4). *, $p<0.01$.

expression in hASCs (data not shown), suggesting that periostin may not be implicated in hASC-stimulated secretion of angiogenic factors and tumor angiogenesis. Accumulating evidence suggests that high expression of periostin is associated with tumorigenesis, metastasis, and angiogenesis in various carcinoma types [25]. Periostin deposition was observed in cancer-associated stroma in various cancer types, including lung and colon [27,49,50]. Bone metastases from breast cancer induced over-expression of periostin by surrounding stromal cells [51]. Periostin has been reported to support adhesion of various carcinoma cells, including ovarian, breast, colon, and oral cancer through an integrin-dependent mechanism [52–55]. Taken together, these results suggest that hASCs stimulate tumor growth through secretion of not only angiogenic factors but also periostin.

Acknowledgements

Grant support: This research was supported by a program through the National Research Foundation of Korea (NRF) funded by the Ministry of Education, Science and Technology (2010-0020274) and by the MRC program of MOST/KOSEF (2010-0001251).

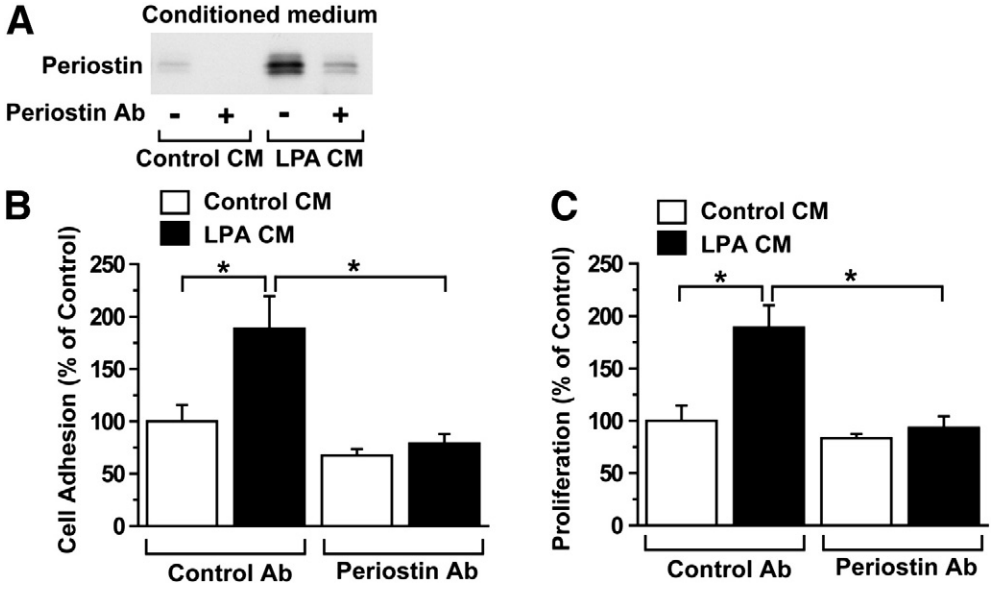

Fig. 6. Effects of periostin immunodepletion on LPA CM-stimulated adhesion and proliferation of A549 cells. (A) LPA CM or control CM were incubated with protein A agarose immobilized with anti-periostin (+) or control (−) antibodies for immunodepletion of periostin and protein levels of periostin in supernatants of conditioned medium after immunoprecipitation were determined by Western blotting. (B) 96-well plates were coated with periostin-depleted (periostin Ab) or mock-treated (control Ab) conditioned medium, and adhesion of A549 cells onto the plates was determined. (C) A549 cells were treated with periostin-depleted (periostin Ab) or control antibody-incubated (control Ab) conditioned medium for 4 days and proliferation of A549 cells was determined. Data are expressed as mean ± SD (n = 4). *, $p<0.05$.

Appendix A. Supplementary data

Supplementary data to this article can be found online at doi:10.1016/j.bbamcr.2011.08.004.

References

[1] O. De Wever, M. Mareel, Role of tissue stroma in cancer cell invasion, J. Pathol. 200 (2003) 429–447.
[2] O. De Wever, P. Demetter, M. Mareel, M. Bracke, Stromal myofibroblasts are drivers of invasive cancer growth, Int. J. Cancer 123 (2008) 2229–2238.
[3] A. Orimo, R.A. Weinberg, Stromal fibroblasts in cancer: a novel tumor-promoting cell type, Cell Cycle 5 (2006) 1597–1601.
[4] A.P. Sappino, O. Skalli, B. Jackson, W. Schurch, G. Gabbiani, Smooth-muscle differentiation in stromal cells of malignant and non-malignant breast tissues, Int. J. Cancer 41 (1988) 707–712.
[5] R. Ganss, Tumor stroma fosters neovascularization by recruitment of progenitor cells into the tumor bed, J. Cell. Mol. Med. 10 (2006) 857–865.
[6] A.F. Olumi, G.D. Grossfeld, S.W. Hayward, P.R. Carroll, T.D. Tlsty, G.R. Cunha, Carcinoma-associated fibroblasts direct tumor progression of initiated human prostatic epithelium, Cancer Res. 59 (1999) 5002–5011.
[7] A. Orimo, P.B. Gupta, D.C. Sgroi, F. Arenzana-Seisdedos, T. Delaunay, R. Naeem, V.J. Carey, A.L. Richardson, R.A. Weinberg, Stromal fibroblasts present in invasive human breast carcinomas promote tumor growth and angiogenesis through elevated SDF-1/CXCL12 secretion, Cell 121 (2005) 335–348.
[8] H. Li, X. Fan, J. Houghton, Tumor microenvironment: the role of the tumor stroma in cancer, J. Cell. Biochem. 101 (2007) 805–815.
[9] F.P. Barry, J.M. Murphy, Mesenchymal stem cells: clinical applications and biological characterization, Int. J. Biochem. Cell Biol. 36 (2004) 568–584.
[10] D.J. Prockop, Marrow stromal cells as stem cells for nonhematopoietic tissues, Science 276 (1997) 71–74.
[11] M.F. Pittenger, A.M. Mackay, S.C. Beck, R.K. Jaiswal, R. Douglas, J.D. Mosca, M.A. Moorman, D.W. Simonetti, S. Craig, D.R. Marshak, Multilineage potential of adult human mesenchymal stem cells, Science 284 (1999) 143–147.
[12] B. Short, N. Brouard, T. Occhiodoro-Scott, A. Ramakrishnan, P.J. Simmons, Mesenchymal stem cells, Arch. Med. Res. 34 (2003) 565–571.
[13] M. Crisan, S. Yap, L. Casteilla, C.W. Chen, M. Corselli, T.S. Park, G. Andriolo, B. Sun, B. Zheng, L. Zhang, C. Norotte, P.N. Teng, J. Traas, R. Schugar, B.M. Deasy, S. Badylak, H.J. Buhring, J.P. Giacobino, L. Lazzari, J. Huard, B. Peault, A perivascular origin for mesenchymal stem cells in multiple human organs, Cell Stem Cell 3 (2008) 301–313.
[14] B. Hall, M. Andreeff, F. Marini, The participation of mesenchymal stem cells in tumor stroma formation and their application as targeted-gene delivery vehicles, Handb. Exp. Pharmacol. (2007) 263–283.
[15] W. Zhu, W. Xu, R. Jiang, H. Qian, M. Chen, J. Hu, W. Cao, C. Han, Y. Chen, Mesenchymal stem cells derived from bone marrow favor tumor cell growth in vivo, Exp. Mol. Pathol. 80 (2006) 267–274.
[16] A.E. Karnoub, A.B. Dash, A.P. Vo, A. Sullivan, M.W. Brooks, G.W. Bell, A.L. Richardson, K. Polyak, R. Tubo, R.A. Weinberg, Mesenchymal stem cells within tumour stroma promote breast cancer metastasis, Nature 449 (2007) 557–563.
[17] P.J. Mishra, P.J. Mishra, R. Humeniuk, D.J. Medina, G. Alexe, J.P. Mesirov, S. Ganesan, J.W. Glod, D. Banerjee, Carcinoma-associated fibroblast-like differentiation of human mesenchymal stem cells, Cancer Res. 68 (2008) 4331–4339.
[18] J. Aoki, Mechanisms of lysophosphatidic acid production, Semin. Cell Dev. Biol. 15 (2004) 477–489.
[19] G.B. Mills, W.H. Moolenaar, The emerging role of lysophosphatidic acid in cancer, Nat. Rev. Cancer 3 (2003) 582–591.
[20] F. Gaits, O. Fourcade, F. Le Balle, G. Gueguen, B. Gaige, A. Gassama-Diagne, J. Fauvel, J.P. Salles, G. Mauco, M.F. Simon, H. Chap, Lysophosphatidic acid as a phospholipid mediator: pathways of synthesis, FEBS Lett. 410 (1997) 54–58.
[21] E.S. Jeon, H.J. Moon, M.J. Lee, H.Y. Song, Y.M. Kim, M. Cho, D.S. Suh, M.S. Yoon, C.L. Chang, J.S. Jung, J.H. Kim, Cancer-derived lysophosphatidic acid stimulates differentiation of human mesenchymal stem cells to myofibroblast-like cells, Stem Cells 26 (2008) 789–797.
[22] M.J. Lee, E.S. Jeon, J.S. Lee, M. Cho, D.S. Suh, C.L. Chang, J.H. Kim, Lysophosphatidic acid in malignant ascites stimulates migration of human mesenchymal stem cells, J. Cell. Biochem. 104 (2008) 499–510.
[23] E.S. Jeon, I.H. Lee, S.C. Heo, S.H. Shin, Y.J. Choi, J.H. Park, D.Y. Park, J.H. Kim, Mesenchymal stem cells stimulate angiogenesis in a murine xenograft model of A549 human adenocarcinoma through an LPA1 receptor-dependent mechanism, Biochim. Biophys. Acta 1801 (2010) 1205–1213.
[24] K. Horiuchi, N. Amizuka, S. Takeshita, H. Takamatsu, M. Katsuura, H. Ozawa, Y. Toyama, L.F. Bonewald, A. Kudo, Identification and characterization of a novel protein, periostin, with restricted expression to periosteum and periodontal ligament and increased expression by transforming growth factor beta, J. Bone Miner. Res. 14 (1999) 1239–1249.
[25] Y. Kudo, B.S. Siriwardena, H. Hatano, I. Ogawa, T. Takata, Periostin: novel diagnostic and therapeutic target for cancer, Histol. Histopathol. 22 (2007) 1167–1174.
[26] I. Takanami, T. Abiko, S. Koizumi, Expression of periostin in patients with non-small cell lung cancer: correlation with angiogenesis and lymphangiogenesis, Int. J. Biol. Markers 23 (2008) 182–186.
[27] A. Soltermann, V. Tischler, S. Arbogast, J. Braun, N. Probst-Hensch, W. Weder, H. Moch, G. Kristiansen, Prognostic significance of epithelial–mesenchymal and mesenchymal–epithelial transition protein expression in non-small cell lung cancer, Clin. Cancer Res. 14 (2008) 7430–7437.
[28] L. Hong, H. Sun, X. Lv, D. Yang, J. Zhang, Y. Shi, Expression of periostin in the serum of NSCLC and its function on proliferation and migration of human lung adenocarcinoma cell line (A549) in vitro, Mol. Biol. Rep. 37 (2010) 2285–2293.
[29] K.U. Choi, J.S. Yun, I.H. Lee, S.C. Heo, S.H. Shin, E.S. Jeon, Y.J. Choi, D.S. Suh, M.S. Yoon, J.H. Kim, Lysophosphatidic acid-induced expression of periostin in stromal cells: Prognoistic relevance of periostin expression in epithelial ovarian cancer, Int. J. Cancer 128 (2011) 332–342.
[30] E.S. Jeon, H.Y. Song, M.R. Kim, H.J. Moon, Y.C. Bae, J.S. Jung, J.H. Kim, Sphingosylphosphorylcholine induces proliferation of human adipose tissue-derived mesenchymal stem cells via activation of JNK, J. Lipid Res. 47 (2006) 653–664.
[31] G. Takayama, K. Arima, T. Kanaji, S. Toda, H. Tanaka, S. Shoji, A.N. McKenzie, H. Nagai, T. Hotokebuchi, K. Izuhara, Periostin: a novel component of subepithelial fibrosis of bronchial asthma downstream of IL-4 and IL-13 signals, J. Allergy Clin. Immunol. 118 (2006) 98–104.
[32] K. Inai, R.A. Norris, S. Hoffman, R.R. Markwald, Y. Sugi, BMP-2 induces cell migration and periostin expression during atrioventricular valvulogenesis, Dev. Biol. 315 (2008) 383–396.
[33] W. Wen, E. Chau, L. Jackson-Boeters, C. Elliott, T.D. Daley, D.W. Hamilton, TGF-ss1 and FAK regulate periostin expression in PDL fibroblasts, J. Dent. Res. 89 (2010) 1439–1443.
[34] J.W. Choi, D.R. Herr, K. Noguchi, Y.C. Yung, C.W. Lee, T. Mutoh, M.E. Lin, S.T. Teo, K.E. Park, A.N. Mosley, J. Chun, LPA receptors: subtypes and biological actions, Annu. Rev. Pharmacol. Toxicol. 50 (2010) 157–186.
[35] E.S. Jeon, S.C. Heo, I.H. Lee, Y.J. Choi, J.H. Park, K.U. Choi, D.Y. Park, D.S. Suh, M.S. Yoon, J.H. Kim, Ovarian cancer-derived lysophosphatidic acid stimulates secretion of VEGF and stromal cell-derived factor-1 alpha from human mesenchymal stem cells, Exp. Mol. Med. 42 (2010) 280–293.
[36] S. Okudaira, H. Yukiura, J. Aoki, Biological roles of lysophosphatidic acid signaling through its production by autotaxin, Biochimie 92 (2010) 698–706.
[37] M. Umezu-Goto, Y. Kishi, A. Taira, K. Hama, N. Dohmae, K. Takio, T. Yamori, G.B. Mills, K. Inoue, J. Aoki, H. Arai, Autotaxin has lysophospholipase D activity leading to tumor cell growth and motility by lysophosphatidic acid production, J. Cell Biol. 158 (2002) 227–233.
[38] M.L. Stracke, H.C. Krutzsch, E.J. Unsworth, A. Arestad, V. Cioce, E. Schiffmann, L.A. Liotta, Identification, purification, and partial sequence analysis of autotaxin, a novel motility-stimulating protein, J. Biol. Chem. 267 (1992) 2524–2529.
[39] S.Y. Yang, J. Lee, C.G. Park, S. Kim, S. Hong, H.C. Chung, S.K. Min, J.W. Han, H.W. Lee, H.Y. Lee, Expression of autotaxin (NPP-2) is closely linked to invasiveness of breast cancer cells, Clin. Exp. Metastasis 19 (2002) 603–608.
[40] Y. Kishi, S. Okudaira, M. Tanaka, K. Hama, D. Shida, J. Kitayama, T. Yamori, J. Aoki, T. Fujimaki, H. Arai, Autotaxin is overexpressed in glioblastoma multiforme and contributes to cell motility of glioblastoma by converting lysophosphatidylcholine to lysophosphatidic acid, J. Biol. Chem. 281 (2006) 17492–17500.
[41] M. Emura, A. Ochiai, M. Horino, W. Arndt, K. Kamino, S. Hirohashi, Development of myofibroblasts from human bone marrow mesenchymal stem cells cocultured with human colon carcinoma cells and TGF beta 1, In Vitro Cell. Dev. Biol. Anim. 36 (2000) 77–80.
[42] N.C. Direkze, K. Hodivala-Dilke, R. Jeffery, T. Hunt, R. Poulsom, D. Oukrif, M.R. Alison, N.A. Wright, Bone marrow contribution to tumor-associated myofibroblasts and fibroblasts, Cancer Res. 64 (2004) 8492–8495.
[43] G. Ishii, T. Sangai, T. Oda, Y. Aoyagi, T. Hasebe, N. Kanomata, Y. Endoh, C. Okumura, Y. Okuhara, J. Magae, M. Emura, T. Ochiya, A. Ochiai, Bone-marrow-derived myofibroblasts contribute to the cancer-induced stromal reaction, Biochem. Biophys. Res. Commun. 309 (2003) 232–240.
[44] M. Erkan, J. Kleeff, A. Gorbachevski, C. Reiser, T. Mitkus, I. Esposito, T. Giese, M.W. Buchler, N.A. Giese, H. Friess, Periostin creates a tumor-supportive microenvironment in the pancreas by sustaining fibrogenic stellate cell activity, Gastroenterology 132 (2007) 1447–1464.
[45] B.M. Beckermann, G. Kallifatidis, A. Groth, D. Frommhold, A. Apel, J. Mattern, A.V. Salnikov, G. Moldenhauer, W. Wagner, A. Diehlmann, R. Saffrich, M. Schubert, A.D. Ho, N. Giese, M.W. Buchler, H. Friess, P. Buchler, I. Herr, VEGF expression by mesenchymal stem cells contributes to angiogenesis in pancreatic carcinoma, Br. J. Cancer 99 (2008) 622–631.
[46] L. Prantl, F. Muehlberg, N.M. Navone, Y.H. Song, J. Vykoukal, C.J. Logothetis, E.U. Alt, Adipose tissue-derived stem cells promote prostate tumor growth, Prostate 70 (2010) 1709–1715.
[47] F.L. Muehlberg, Y.H. Song, A. Krohn, S.P. Pinilla, L.H. Droll, X. Leng, M. Seidensticker, J. Ricke, A.M. Altman, E. Devarajan, W. Liu, R.B. Arlinghaus, E.U. Alt, Tissue-resident stem cells promote breast cancer growth and metastasis, Carcinogenesis 30 (2009) 589–597.
[48] K. Shinagawa, Y. Kitadai, M. Tanaka, T. Sumida, M. Kodama, Y. Higashi, S. Tanaka, W. Yasui, K. Chayama, Mesenchymal stem cells enhance growth and metastasis of colon cancer, Int. J. Cancer 127 (2010) 2323–2333.
[49] N. Fukushima, Y. Kikuchi, T. Nishiyama, A. Kudo, M. Fukayama, Periostin deposition in the stroma of invasive and intraductal neoplasms of the pancreas, Mod. Pathol. 21 (2008) 1044–1053.
[50] Y. Kikuchi, T.G. Kashima, T. Nishiyama, K. Shimazu, Y. Morishita, M. Shimazaki, I. Kii, H. Horie, H. Nagai, A. Kudo, M. Fukayama, Periostin is expressed in pericryptal fibroblasts and cancer-associated fibroblasts in the colon, J. Histochem. Cytochem. 56 (2008) 753–764.
[51] S. Contie, N. Voorzanger-Rousselot, J. Litvin, P. Clezardin, P. Garnero, Increased expression and serum levels of the stromal cell-secreted protein periostin in breast cancer bone metastases, Int. J. Cancer 128 (2011) 352–360.
[52] S. Bao, G. Ouyang, X. Bai, Z. Huang, C. Ma, M. Liu, R. Shao, R.M. Anderson, J.N. Rich, X.F. Wang, Periostin potently promotes metastatic growth of colon cancer by augmenting cell survival via the Akt/PKB pathway, Cancer Cell 5 (2004) 329–339.

[53] Y. Kudo, I. Ogawa, S. Kitajima, M. Kitagawa, H. Kawai, P.M. Gaffney, M. Miyauchi, T. Takata, Periostin promotes invasion and anchorage-independent growth in the metastatic process of head and neck cancer, Cancer Res. 66 (2006) 6928–6935.
[54] R. Shao, S. Bao, X. Bai, C. Blanchette, R.M. Anderson, T. Dang, M.L. Gishizky, J.R. Marks, X.F. Wang, Acquired expression of periostin by human breast cancers promotes tumor angiogenesis through up-regulation of vascular endothelial growth factor receptor 2 expression, Mol. Cell. Biol. 24 (2004) 3992–4003.
[55] L. Gillan, D. Matei, D.A. Fishman, C.S. Gerbin, B.Y. Karlan, D.D. Chang, Periostin secreted by epithelial ovarian carcinoma is a ligand for alpha(V)beta(3) and alpha(V)beta(5) integrins and promotes cell motility, Cancer Res. 62 (2002) 5358–5364.